A phenomenological study of the structural relaxation of poly(methyl methacrylate)

J. L. Gómez Ribelles, A. Ribes Greus and R. Díaz Calleja
Laboratory of Thermodynamics and Physical-Chemistry, ETSII, Universidad Politecnica de Valencia, PO Box 22012, 46071 Valencia, Spain
(Received 20 October 1988; revised 2 May 1989; accepted 2 May 1989)

The structural relaxation process of poly(methyl methacrylate) has been studied by differential scanning calorimetry. The sample was subjected to different thermal histories with isothermal stages at ageing temperatures of 100 and 80°C for different ageing times. The enthalpy increment suffered by the sample in the isothermal stage of the thermal history (enthalpy loss due to ageing) was calculated as a function of the ageing time and temperature. The specific heat curves measured were fitted to two phenomenological models.

(Keywords: structural relaxation; poly(methyl methacrylate); thermal history)

INTRODUCTION

Structural relaxation is the process by which amorphous materials in the glassy state approach a state of thermodynamic equilibrium. This process is detected through the time evolution of thermodynamic properties such as specific volume or enthalpy[1,2], as well as mechanical[3,4] or dielectric[5,6] properties. The study of structural relaxation in amorphous polymers by means of differential scanning calorimetry (d.s.c.) deserves more attention because of the high reproducibility of the thermal histories of the experiments and the simplicity of the experimental procedure. This explains why the number of experimental works that use this technique is now greater than those using dilatometric measurements.

A polymer sample is subjected to a more or less complicated thermal history, which starts at a temperature T_0 (higher than the glass transition temperature, T_g), with the sample in thermodynamic equilibrium, and involves stages with heating or cooling at constant rates as well as isothermal stages, finishing at a temperature T_1 in the glassy state. Then, the specific heat at constant pressure is measured during a heating scan at constant rate between T_1 and T_0. The $c_p(T)$ curve thus obtained depends on the thermal history of the sample and contains information about structural relaxation, which occurs both in the process previous to the measurement and in the measuring scan itself. In particular, when the thermal history includes an isothermal stage, at a temperature T_a (usually called the ageing temperature) with a duration t_a (called the ageing time), there exist several procedures, more or less accurate, which allow one to determine the enthalpy increment Δh_a suffered by the material in that stage[7-10]. The plot of Δh_a against t_a determines the evolution of enthalpy during the isothermal recovery process at temperature T_a.

The $c_p(T)$ curves measured after isothermal stages at high enough ageing temperatures present a characteristic peak that overlaps the glass transition. However, when T_a is lower, there appears a peak in c_p in a range of temperatures below the glass transition, which then occurs practically as if the thermal history had not included the isothermal stage[11]. The position and height of the maximum depend on T_a and t_a and reflect the non-linearity, asymmetry and memory effect (the latter in particular in the peaks that appear at temperatures below the range of the glass transition), which characterize the structural relaxation process[12].

Several phenomenological models[12-15] have been proposed to describe structural relaxation from a macroscopic point of view. The models are based on the idea of the existence of a distribution of recovery times, which evolves when the temperature and/or the separation from equilibrium change. Several adjustable parameters determine the shape and position on the temperature axis of the distribution of recovery times.

In this work, the structural relaxation process in atactic poly(methyl methacrylate) (PMMA) has been studied at two temperatures, 100 and 80°C. The first of these is high enough to obtain peaks in c_p overlapping the high-temperature side of the glass transition, and the second is low enough to produce maxima in c_p within the range of temperatures of the glass transition. The applicability of two phenomenological models has been analysed.

EXPERIMENTAL

The sample was prepared by radical polymerization of the monomer, from Merck, previously distilled. Azobisisobutyronitrile (0.06%) was used as initiator. The polymerization took place at 60°C for 14 h and the sample was then dried to constant weight at 70°C in a vacuum. A sample of 6 mg of polymer was sealed in an aluminium pan and used in all the measurements.

A Perkin–Elmer DSC4 differential scanning calorimeter with a data station model 3600 was used in this work, collecting four data points per degree centigrade. All the thermal treatments were carried out in the calorimeter. Three different types of experiments were performed, as outlined below.

(A) The sample was annealed at 150°C for 10 min to ensure that it is in equilibrium and so to eliminate the

0032-3861/90/020223-08$03.00

effect of previous thermal histories. The sample was then cooled at 40°C min^{-1} to temperature T_a, kept at this temperature for time t_a and cooled again at 40°C min^{-1} until $T_1 = 40$°C, the temperature selected for the start of the measuring scan, which took place by heating at 20°C min^{-1} until 150°C. The measuring scan was then repeated with an empty pan in place of the sample pan. From these two measurements, the specific heat of the polymer was calculated between 60 and 150°C. The calorimeter was frequently calibrated with a sapphire standard.

The $c_p(T)$ curve measured after an experiment with $t_a \neq 0$ will be called hereafter an ageing scan ($c_{p,a}(T)$) and the one with $t_a = 0$ a reference scan ($c_{p,ref}(T)$). Four reference scans were measured and an average used in this work.

(B) In order to increase the accuracy of the calculation of Δh_a, which involves the difference between an ageing scan and a reference scan, a series of experiments were carried out in which, after the first measuring scan in the calorimeter (without performing the empty pan scan and after annealing at 150°C for 10 min), the sample was cooled at 40°C min^{-1} to $T_1 = 40$°C and then subjected to a new measuring scan. The difference between both scans allows one to determine the curve $c_{p,a}(T) - c_{p,ref}(T)$. In this way the conditions of measuring the ageing and reference scans are exactly the same.

(C) A series of experiments were performed in order to use the method proposed by Lagasse[7] for the calculation of Δh_a. The sample was annealed at 150°C for 10 min, cooled down at 40°C min^{-1} to T_a and kept at this temperature for time t_a; then the measuring scan was carried out between T_a and 150°C at 20°C min^{-1}. Another measuring scan followed with $t_a = 0$. The description and analysis of the results of these experiments will be given below.

RESULTS AND DISCUSSION

Phenomenological models of structural relaxation

The experimental curves of ageing experiments are usually presented in terms of the fictive temperature T_f, which, following an idea of Tool[16], attempts to associate an equilibrium state to each out-of-equilibrium state and also to normalize the specific heat curves. It can be proven[17] that T_f can be deduced from the equation:

$$\int_{T_f}^{T^*} (c_{p,l} - c_{p,g})\,dT = \int_{T}^{T^*} (c_{p,a} - c_{p,g})\,dT \qquad (1)$$

where $c_{p,l}(T)$ and $c_{p,g}(T)$ are respectively the specific heats of the polymer in the liquid and glassy states. From (1) it follows that:

$$\frac{dT_f}{dT} = \frac{(c_{p,a} - c_{p,g})(T)}{(c_{p,l} - c_{p,g})(T_f)} \qquad (2)$$

The dT_f/dT curves are equivalent to a normalized specific heat since in equilibrium $dT_f/dT = 1$ and in the glassy state T_f does not depend on the temperature and $dT_f/dT = 0$.

Figure 1 shows the curves calculated from the results of experiments of type A. The curves obtained after thermal histories that include an isothermal ageing at 100°C show only a maximum that overlaps the high-temperature side of the transition. It must be noted that the reference scan also shows a small peak at a

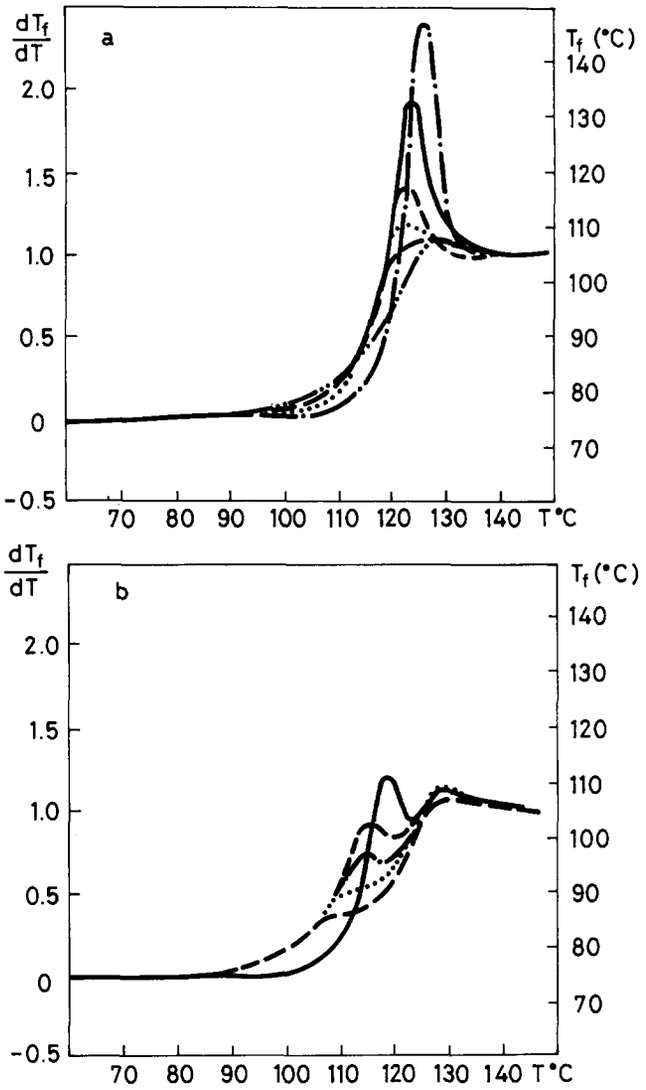

Figure 1 Curves of dT_f/dT measured after different thermal histories involving an isothermal stage at temperature T_a for a time t_a. (a) $T_a = 100$°C; (-·-·-·-) $t_a = 0$; (–––) $t_a = 15$ min; (·····) $t_a = 30$ min; (------) $t_a = 75$ min; (——) $t_a = 150$ min; (-·-·-) $t_a = 835$ min. (b) $T_a = 80$°C; (–––) $t_a = 50$ min; (·····) $t_a = 135$ min; (-·-·-) $t_a = 390$ min; (------) $t_a = 975$ min; (——) $t_a = 3800$ min

temperature of ~130°C, due to the stages of cooling and heating. This peak is hidden in the ageing curves at least with t_a longer than 15 min. In the curves obtained after ageing at 80°C there appears a peak at temperatures within the temperature range of the glass transition, and another one identical to that appearing in the reference scan. As in the ageing at 100°C, the maximum shifts towards higher temperatures when the ageing time increases, but the peak due to the isothermal stage never overlaps that of the reference scan. The low-temperature peaks are related to the memory effect, as they reflect a recovery of enthalpy in the opposite direction to the approach to equilibrium[15]. Thus the behaviour at these two ageing temperatures is diverse enough to give a quite complete description of the structural relaxation process.

The enthalpy recovery that follows a sudden change in temperature, from T^* in time t_0 with the material in equilibrium to T_a, can be described phenomenologically by means of a decay function $\varphi(t, t_0)$:

$$\frac{h(T_a, t_a) - h^{eq}(T_a)}{h(T_a, 0) - h^{eq}(T_a)} = \frac{T_f - T_a}{T^* - T_a} = \varphi(t, t_0) \qquad (3)$$

The nomenclature is given in *Figure 5* below. Several models assume for $\varphi(t, t_0)$ an equation of Williams–Watts[18] type:

$$\varphi(t, t_0)=\exp\left[-\left(\int_{t_0}^{t} \mathrm{d}t/\tau\right)^{\beta}\right] \quad (4)$$

where

$$\tau=\tau(T, T_f(t)) \quad (5)$$

The parameter β and the double dependence of τ on T and T_f allows the model to reproduce the essential characteristics found experimentally in structural relaxation: non-linearity, asymmetry and memory effect[12].

The material response to a complex thermal history that involves stages of heating or cooling at constant rate has been modelled in this work by approaching these stages by means of a series of successive steps in temperature, each one of 1°C, with intermediate isothermal periods, reproducing on average a rate of change of temperature equal to the experimental one. Equation (3) is linearized by the change of variable:

$$\xi=\int_{t_0}^{t} \mathrm{d}t/\tau$$

used[13,14] to apply the superposition principle to the response to the different steps.

Different expressions have been proposed for equation (5)[6,13–15]. Two of them will be applied in this work. The one proposed by Narayanaswamy[13] (called hereafter the N model) can be expressed[14] as:

$$\tau=A\ \exp(\Delta h^*/R)[x/T+(1-x)/T_f)] \quad (6)$$

The AGV model proposed by Hodge[15] is given by:

$$\tau=A\ \exp\{D/[RT(1-T_2/T_f)]\} \quad (7)$$

Both models involve four adjustable parameters, which were adjusted by a least-squares fit, following the search routine of Nedler and Mead[19].

The pre-exponential factor A attains very high values, mainly in the N model, which predicts an Arrhenius behaviour for the equilibrium relaxation times, instead of the Williams–Landel–Ferry or Vogel behaviour found by means of viscoelastic or dielectric relaxation in this range of temperatures. Thus the N model is able to fit correctly the experiments but the A parameter has no physical meaning.

A reference temperature T_R was defined as the temperature at which the relaxation time in equilibrium is 1 s. This temperature is a bit higher than T_g and is more useful for the analysis of the results. The parameter A was calculated from T_R through:

$$\ln A=(-\Delta h^*)/RT_R$$

in the N model and through:

$$\ln A=-D/R(T_R-T_2)$$

in the AGV model. The use of T_R instead of A does not change the model at all.

The AGV model

Not all parameters in the phemenological models with four parameters seem to be independent; the least-squares fit of an experimental curve usually has several solutions with different sets of parameters but very small differences in the standard deviation.

This forces us to calculate one of the parameters in an independent way if possible, or to postulate its value more or less arbitrarily.

In this work the calculation routine was the following. The first targets of the modelling were the $\mathrm{d}T_f/\mathrm{d}T$ curves measured after thermal histories with ageing at 100°C for 835 min and at 80°C for 3800 min, the longest ageing times and so the curves with the most prominent peaks, which could be the most significant.

Keeping D fixed, the other three parameters were adjusted, attaining a very good fit to the experimental results. Different values of D higher than 5 kcal mol^{-1} were found to allow a similar fit to the experimental results but with values of β, T_2 and T_R that depend on the fixed value of D (see *Table 1*). T_2 is the parameter that shows the strongest correlation with D, with values separated by as much as 40°C when D varies between 5 and 11 kcal mol^{-1}. The values of β and T_R depend only slightly on D.

The correlation between D and T_2 is also apparent in a plot of the values of τ corresponding to equilibrium ($T_f=T$):

$$\tau^{eq}=A\ \exp[(D/R)/(T-T_2)]$$

against $1/T$. The equilibrium curves calculated with the different pairs of D and T_2 found practically overlap in the range of temperatures of the ageing experiments. In this sense the dependence of T_2 with D in the model has no great conceptual importance because the physical magnitude controlled by these two parameters is nearly unequivocally defined.

A more important problem is the fact that the parameters determined by the fit of experimental curves measured after different thermal histories are different, and with them the τ^{eq} curves that they define. Thus for the same values of D the value of T_2 is significantly higher when determined for curves with ageing at 80°C than with ageing at 100°C (*Table 1*). Also small differences in β and T_2 are found. *Figure 3* shows the interval of variation of the τ^{eq} curves defined by the parameters calculated from the different thermal histories. The values of the average relaxation times calculated from dielectric measurements (from curves of ε'', the imaginary part of the complex dielectric permittivity, against temperature[20]) are also presented. The difference in the slope of the log τ^{eq} vs. $1/T$ curve is quite apparent and cannot be justified at present.

A value of $D=8$ kcal mol^{-1} was arbitrarily selected to adjust the rest of the experimental curves. Systematic dependences appear in the other three parameters with ageing time and temperature, again mainly in T_2 as shown in *Table 2*. In *Figure 2* the curves predicted by the model for several experimental thermal histories have been presented.

The N model

The Narayanaswamy model has been perhaps the most used so far, showing a precise description of the experimental results in different materials[13,14,21,22]. As mentioned above, a close relation between x and Δh^* has been reported in the literature, and leads one to calculate Δh^* from the dependence of the value of T_f in the glassy state with the cooling rate. The value of Δh^* thus calculated is always very high. In this work an adjustment routine similar to that used with the AGV model has been preferred. Different values of Δh^* were

Table 1 Parameters of the AGV model that give the best fit to the experimental curves defined by T_a and t_a. The value of D was kept fixed in the search routine with the tabulated values. $\hat{\sigma}^2$ is the residual error variance

T_a (°C)	t_a (min)	D (kcal mol^{-1})	β	T_2 (°C)	T_R (°C)	$\hat{\sigma}^2$
100	835	4	0.30	44.4	125.7	0.0337
100	835	5	0.29	45.9	126.2	0.0144
100	835	6	0.30	43.5	126.7	0.0110
100	835	7	0.30	38.9	126.6	0.0109
100	835	8	0.31	32.3	126.7	0.0104
100	835	9	0.31	27.3	127.0	0.0102
100	835	11	0.32	16.0	127.0	0.0106
100	835	15	0.35	5.0	127.0	0.0100
80	3800	5	0.31	69.8	124.0	0.0037
80	3800	6	0.32	64.1	124.1	0.0028
80	3800	7	0.32	55.6	124.2	0.0024
80	3800	8	0.33	50.5	124.5	0.0015
80	3800	9	0.34	45.3	124.8	0.0015
80	3800	11	0.34	32.6	125.3	0.0013

Table 2 Parameters of the AGV model giving the best fit to the experimental curves. The paramete D was kept fixed with a value of 8 kcal mol^{-1}

T_a (°C)	t_a (min)	β	T_a (°C)	T_R (°C)	$\hat{\sigma}^2$
100	835	0.31	32.3	126.7	
100	150	0.33	35.8	126.3	0.0058
100	75	0.33	38.4	125.9	0.0022
100	30	0.36	43.2	124.3	0.0009
100	15	0.36	38.8	125.3	0.0003
	0	0.34	40.0	124.0	0.0003
80	3800	0.33	50.5	124.5	0.0015
80	975	0.34	47.3	124.1	0.0032
80	390	0.33	40.8	124.5	0.0020
80	135	0.36	39.4	124.3	0.0027
80	50	0.28	44.0	125.0	0.0004

checked in the curves measured after the thermal histories with the longest ageing times.

Table 3 shows that an increase in Δh^* leads to a decrease in both x and β parameters. The characteristic peak in dT_f/dT narrows. So for values of Δh^* higher than 150 kcal mol^{-1} the standard deviation increases rapidly. In ageing curves with $T_a = 80$°C the effect is similar but now the best fit is attained with a value of Δh^* around 250 kcal mol^{-1}. With higher values of Δh^* the high-temperature side of the dT_f/dT curve rapidly separates from the experimental one, although the area of the peak can be still more or less fitted.

For the other thermal histories a value of $\Delta h^* = 200$ kcal mol^{-1} was selected (*Table 4*). Now the parameter x shows a more significant dependence on the ageing time, ranging between 0.15 and 0.26. The values of the parameters β and T_R are a bit scattered in this model because its accuracy is slightly less than in the AGV model.

Figure 3 shows the equilibrium recovery time curve:

$$\tau^{eq} = A \exp(\Delta h^*/RT)$$

The straight line predicted in the $\ln \tau^{eq}$ vs. $1/T$ plots is similar, in the temperature range of ageing experiments, to the curves found in the AGV model.

Several authors have already found systematic changes in the parameters of phenomenological models with thermal history[20,21] that are difficult to explain in the framework of the theory. Nevertheless, the excellent fit to the experimental curves is notorious with both models. The importance of the changes in the model parameters can be seen by comparing the curves predicted by the model for the different thermal histories using the same set of parameters for all of them.

Figure 4 shows this plot using an average of the parameters found previously. Both models reproduce the experimental behaviour qualitatively and quantitatively well, although as expected the fit is worse than in *Figure 2*. Both models tend to predict narrower peaks than the experimental ones in curves with ageing temperature of 100°C. Small shifts in temperature and height of the peaks are also detected.

Enthalpy recovery process

The method used for the calculation of the enthalpy increment that takes place during the isothermal stage of the thermal history is based on the scheme shown in *Figure 5*. The full curve schematizes the specific enthalpy of the polymer as a function of temperature for an experiment of type A. The enthalpy increment in the isothermal stage is:

$$\Delta h_a = h(T_a, 0) - h(T_a, t_a)$$

It can be easily deduced that:

$$h_0 - h_{0'} = \int_{T_1}^{T^*} (C_{p,a} - C_{p,ref})\, dT$$

T^* is a temperature high enough to accept that the polymer is in equilibrium.

If it is possible to assume that the lines AO and CO' in *Figure 5* are parallel, $\Delta h_a = (h_0 - h_{0'})$, and it can be calculated by means of the shaded area in *Figure 5*.

Figure 6 represents an experimental curve of the C_p difference between an ageing and a reference scan. This curve attains negative values between 60 and 120°C and positive values at higher temperatures, showing the characteristic ageing peak. It is notorious that the negative part extends to temperatures below the ageing temperature, a fact found in all the experiments of type A and B and for the two ageing temperatures used.

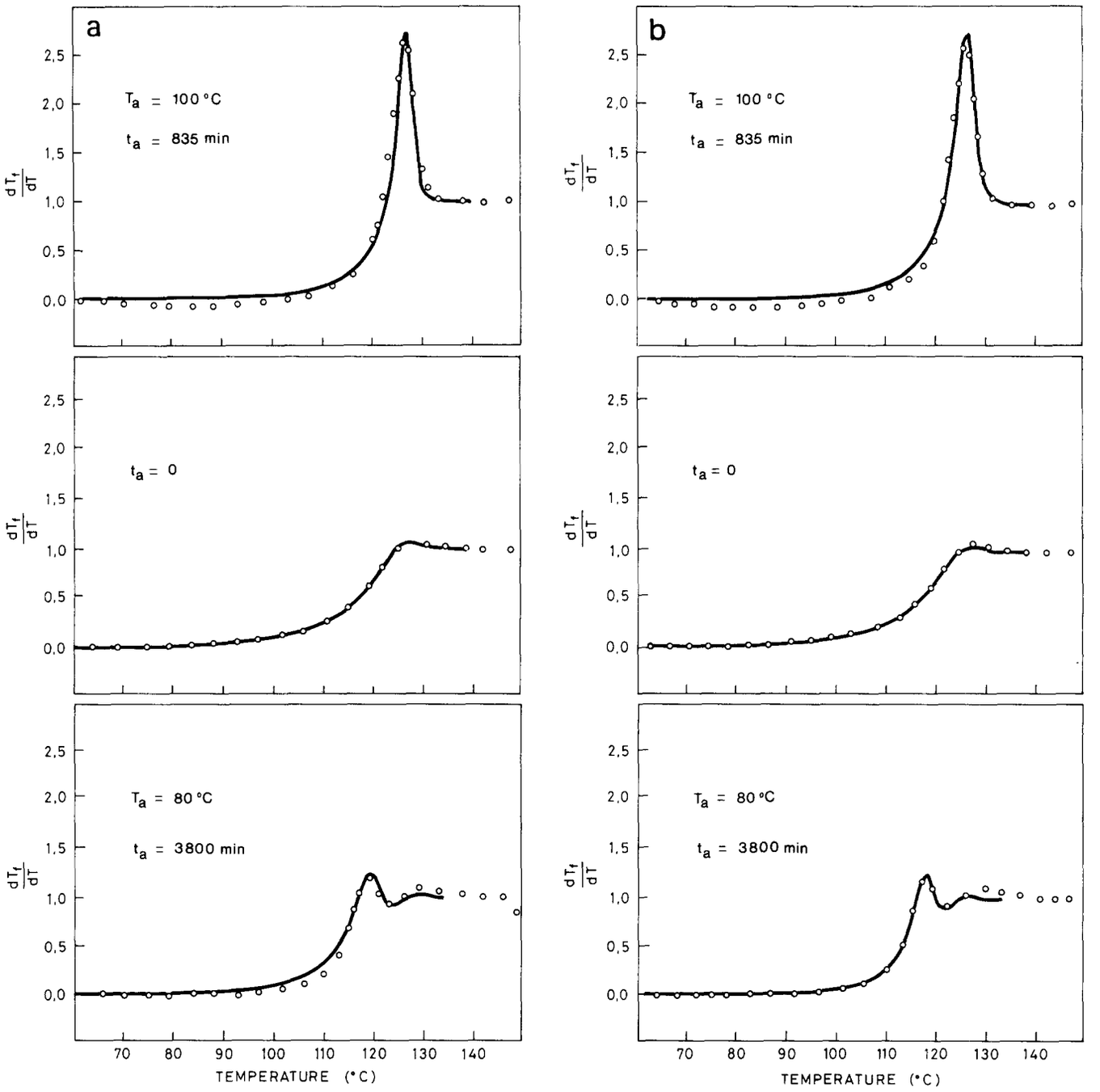

Figure 2 Curves of dT_f/dT predicted by the two phenomenological models. The full curve represents the best fit found for each thermal history, characterized by T_a and t_a given on the graph. The parameters of the models are given in *Tables 2* and *Figure 4*. The experimental data are represented by open circles; not all the experimental points are shown for the sake of clarity. (a) AGV model; (b) N model

Table 3 Parameters of the N model that give the best fit to the experimental curves defined by T_a and t_a. The value of Δh^* was kept fixed in the search routine with the tabulated values. $\hat{\sigma}^2$ is the residual error variance

T_a (°C)	t_a (min)	Δh^* (kcal mol^{-1})	β	x	T_R (°C)	$\hat{\sigma}^2$
100	835	125	0.66	0.73	129.2	0.0057
100	835	150	0.41	0.46	127.1	0.0078
100	835	200	0.32	0.26	126.7	0.0163
100	835	250	0.34	0.23	126.3	0.0307
100	835	300	0.29	0.16	126.2	0.0531
80	3800	150	0.37	0.39	128.4	0.0055
80	3800	200	0.33	0.26	125.8	0.0036
80	3800	250	0.33	0.21	124.5	0.0017
80	3800	300	0.35	0.18	122.6	0.0019

Table 4 Parameters of the N model giving the best fit to the experimental curves. The parameter Δh^* was kept fixed with a value of 200 kcal mol^{-1}

T_a (°C)	t_a (min)	β	x	T_R (°C)	$\hat{\sigma}^2$
100	835	0.32	0.26	126.7	0.0164
100	150	0.31	0.18	125.3	0.0086
100	75	0.31	0.19	125.8	0.0035
100	30	0.37	0.25	124.3	0.0008
100	15	0.33	0.18	125.0	0.0008
	0	0.35	0.15	124.2	0.0003
80	3800	0.32	0.26	126.3	0.0037
80	975	0.36	0.26	125.3	0.0043
80	390	0.32	0.23	124.4	0.0020
80	135	0.36	0.22	124.2	0.0031
80	50	0.31	0.21	125.8	0.0002

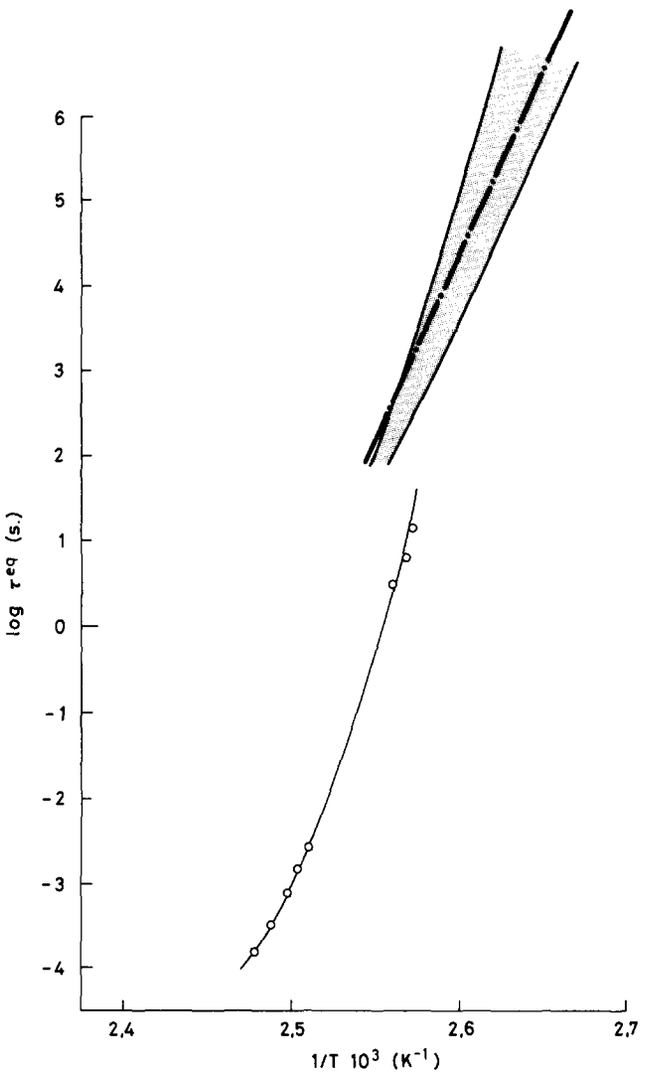

Figure 3 Equilibrium recovery times τ_0^{eq} predicted by the models. In the AGV model the curves calculated from the different thermal histories fall within the shaded area limited by the curves defined by the sets of parameters $T_R = 126.7$°C, $T_2 = 32.3$°C, $D = 8$ kcal mol^{-1} and $T_R = 124.5$°C, $T_2 = 50.5$°C, $D = 8$ kcal mol^{-1} (see *Table 2*). In the N model the τ_0^{eq} predicted is shown by the chain line. The values of the average relaxation time calculated from dielectric results are also represented (○)

This implies that, in the cooling process between T_a and T_1 and the following heating process between T_1 and T_a, the evolution of enthalpy is greater in the ageing curve than in the unaged one, an unexpected fact since the molecular mobility is lower in the aged sample and so the behaviour of the aged sample should be closer to that of the glass. If this is assumed, the negative values of $C_p - C_{p,ref}$ between 60 and 100°C must be interpreted in the sense that the $C_p(T)$ values in the reference scan are higher than those of the glass in the range of temperatures. So during heating in the unaged sample the evolution of enthalpy is in the opposite direction to the approach to equilibrium and must be interpreted from a phenomenological point of view in terms of the

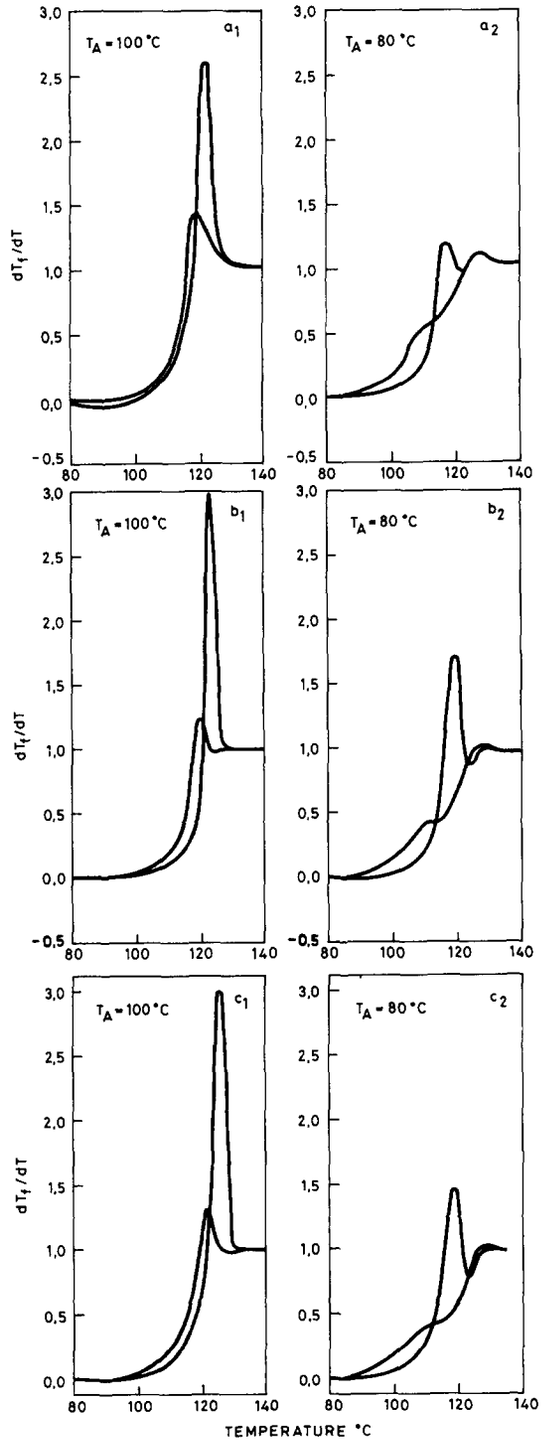

Figure 4 Curves of dT_f/dT predicted by the models using the same set of parameters for the different thermal histories. (a_1) Experimental curves for $T_a = 100$°C, $t_a = 835$ and 75 min. (a_2) Experimental curves for $T_a = 80$°C, $t_a = 3800$ and 135 min. (b_1), (b_2) AGV model with the following set of parameters: $\beta = 0.34$, $T_2 = 45$°C, $D = 8$ kcal mol^{-1}, $T_R = 125$°C. (c_1), (c_2) N model with the following set of parameters: $\beta = 0.33$, $x = 0.25$, $\Delta h^* = 200$ kcal mol^{-1}, $T_R = 125$°C. The thermal histories are the same as in (a_1) and (a_2)

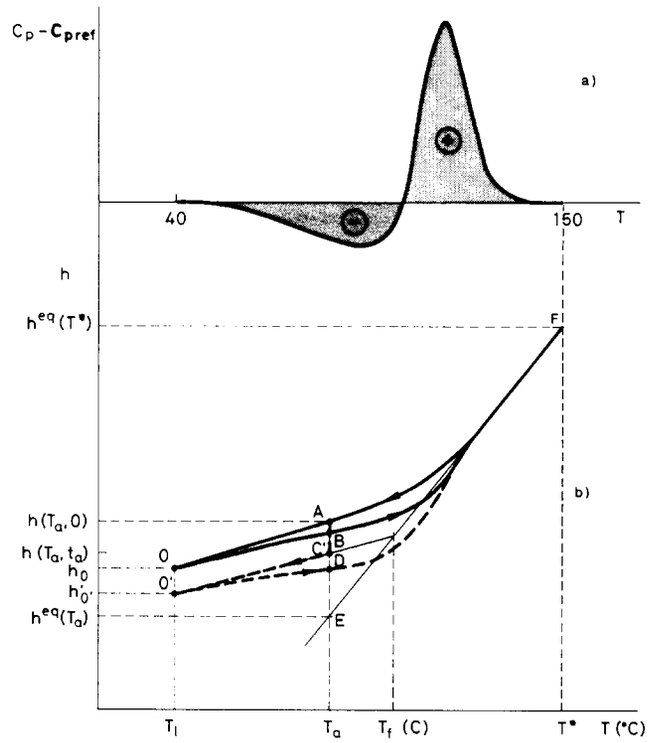

Figure 5 (a) Schematic diagram of the difference between the specific heat measured after a thermal history with and without isothermal ageing – see text. (b) Schematic diagram of the evolution of the specific enthalpy of the sample during a thermal history without isothermal ageing (full curve FAOBF) and another one with isothermal ageing at T_a (broken curve FAC'ODF)

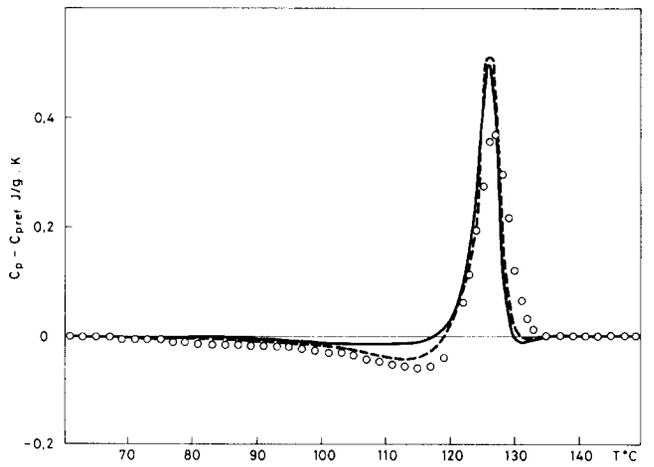

Figure 6 Diagram showing the difference between the specific heat measured after ageing at 100°C for 835 min and the reference scan. The open circles represent the experimental points. The broken curve shows the prediction for this curve of the AGV model and the full curve shows the prediction of the N model. The values of the parameters are given in *Table 2* and *4* respectively

memory effect. In fact the two phenomenological models studied reproduce the experimental facts qualitatively. The model predictions for the curve shown in *Figure 6* were calculated using the same values of the parameters for the ageing and reference scans, the ones which best fit the ageing curve. Both models present a negative part at temperatures below 100°C but with absolute values significantly lower than the experimental ones.

This behaviour forces one to be suspicious of the approximation $\Delta h_a = h_0 - h_{0'}$ at least at ageing temperature $T_a = 100$°C, just 15°C below T_g. For this ageing temperature the method of Lagasse[7] was also used to determine Δh_a (experiments of type C).

An example of the result of this experiment is shown in *Figure 7*. The difference between the heat flux output of the d.s.c. in an ageing ($T_a = 100$°C) and a reference scan is represented against the time elapsed from the start of the measuring scan. For times lower than 0.5 min and higher than 3 min the temperature of the sample is constant and equal to 100 and 150°C, respectively. Two sharp peaks appear at the start and the end of the heating scan due to small shifts in temperature between the two scans (about 0.2°C). As described in ref. 7 the shaded area in *Figure 7* equals Δh_a. (A short extrapolation on the low-temperature side of the curve can avoid the effect of the sharp peaks at the start and the end of the scan, measuring the area only for times corresponding to the heating part of the scan; no difference was found between the two methods of calculation).

The values of Δh_a at 100°C calculated from experiments A and B (conceptually identical) and experiment C are compared in *Figure 8a*. When the ageing time is greater than 100 min a small but systematic difference between both calculation methods is found, which is significant, taking into account that the ageing temperature is not very close to T_g ($T_g - T_a = 15$°C). At $T_a = 80$°C only experiments of type A and B were carried out. The values of Δh_a are represented on *Figure 8b*.

The limit of Δh_a to infinite ageing time, Δh_∞, can be determined from a reference curve, $C_{p,\mathrm{ref}}$, using the equation:

$$\Delta h_\infty = h(T_a, 0) - h^{eq}(T_a) = \int_{T_a}^{T^*} (C_{p,l} - C_{p,\mathrm{ref}})\, dT$$

which follows from the scheme of *Figure 5*. Here $C_{p,l}(T)$ was adjusted to a linear equation determined from an average of four reference scans in the range of temperatures between 105 and 150°C:

$$C_{p,l} = 0.372 + 3.895 \times 10^{-3} T \ \mathrm{J\,g^{-1}\,K^{-1}}$$

The Δh_∞ value was 4.1 J g^{-1} for $T_a = 100$°C and 9.5 J g^{-1} for $T_a = 80$°C. At both temperatures the value is much higher than the experimental ones as found in other polymers[10,23], which implies that the experimental range of ageing times only covers the initial part of the enthalpy recovery curve or that the equilibrium state determined by extrapolation of the liquid behaviour is not correct.

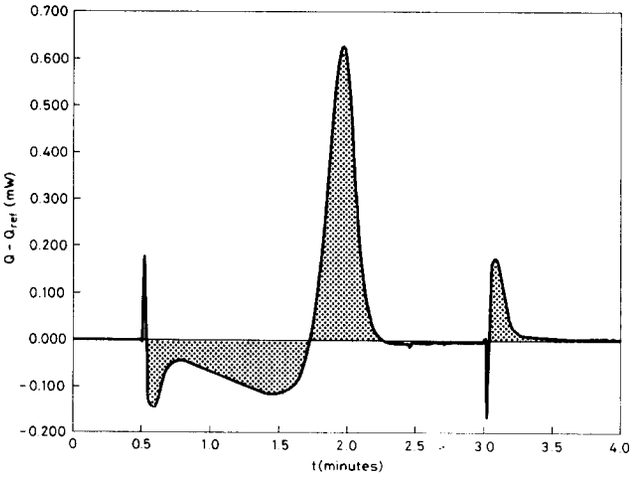

Figure 7 Difference between the heat flux measured after ageing at 100°C for 3800 min and after a thermal history without isothermal ageing. According to the Lagasse method, the shaded area allows one to calculate Δh_a

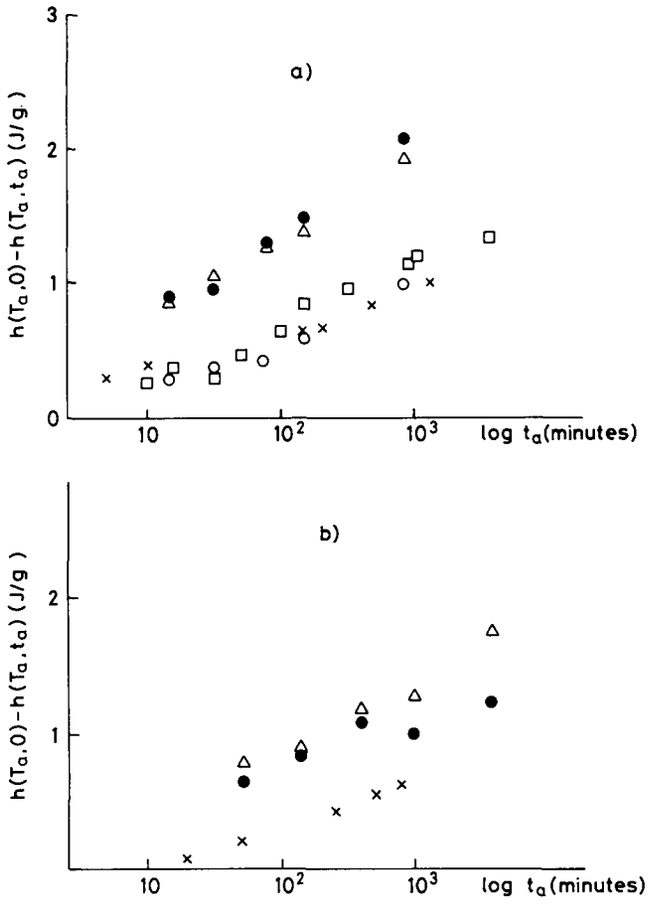

Figure 8 Enthalpy increment in the isothermal ageing at (a) $T_a = 100°C$ and (b) $T_a = 80°C$: (×) results of experiments of type A; (○) results of experiments of type B; (□) results of experiments of type C; (●) predictions of the AGV model; (△) predictions of the N model

The values of Δh_a were also calculated by means of two phenomenological models, both predicting values noticeably higher than the experimental ones (*Figure 8*), which may be related to the difficulty in reproducing the negative part of the $(C_p - C_{p,ref}(T))$ curve.

The phenomenological models used in this work rely on two basic ideas. First, there exists a spectrum of areas of the material which relax with different rates; these areas may be associated with a distribution in free volume or, in general, with a distribution in the characteristics of the neighbourhoods of the molecular groups that relax. Secondly, it is assumed that the structural relaxation process would finish, after infinite time, in an equilibrium state in which the enthalpy of the material $h^{eq}(T)$ is the one determined by the extrapolation of the $h(T)$ curve measured at temperatures above T_g.

This concept of the material reproduces the general features of the structural relaxation phenomenon but there are several details that lead one to think that physical reality is not as simple as that of the model. The difficulty of the model in describing the low-temperature side of the $c_p(T)$ curves and the enthalpy lost due to ageing may lead one to think that the extrapolation of the equilibrium curve is not correct and that the actual limit of Δh_a for infinite time is less than the theoretical one. The differences between the dielectric relaxation times and the structural relaxation times also make it necessary to rethink the dependence of the recovery times on structure, i.e. the expression for the dependence of the recovery times with T and T_f.

CONCLUSIONS

The two phenomenological models studied reproduce with similar accuracy the dT_f/dT curves measured after different thermal histories. The fit is excellent when the best set of parameters is used for each curve. If only one set of parameters is used for all the curves, the fit is still acceptable but the peaks for long ageing times are narrower than the experimental ones.

The value of Δh_a determined by means of the shaded area in *Figure 5* is slightly different from the one calculated by the Lagasse method (*Figure 7*) at an ageing temperature of 100°C. The differences are ascribed to the fact that the specific heat curves measured after an ageing and a reference scan present small but significant differences at temperatures below the ageing temperature. These differences are qualitatively reproduced by both phenomenological models. The values of Δh_a calculated by the models are much higher than the experimental ones.

ACKNOWLEDGEMENT

The work was partially supported by CAICYT Grant 0493/84.

REFERENCES

1 Kovacs, A. J. *Adv. Polym. Sci.* 1963, **3**, 394
2 Davies, R. O. and Jones, G. O. *Adv. Phys.* 1953, **2**, 370
3 Struik, L. C. E. 'Physical Ageing in Amorphous Polymers and Other Materials', Elsevier, Amsterdam, 1978
4 Petrie, S. E. B. 'Polymeric Materials', American Society for Metals, Ohio, 1973
5 Gómez-Ribelles, J. L. and Díaz-Calleja, R. *Polym. Bull.* 1985, **14**, 45
6 Matsuoka, S. *et al. Macromolecules* 1985, **18**, 2652
7 Lagasse, R. R. *J. Polym. Sci., Polym. Phys. Edn.* 1982, **20**, 279
8 Petrie, S. E. B. *J. Polym. Sci. (A-2)* 1972, **10**, 1255
9 Bauwens-Crowet, C. and Bauwens, J. C. *Polymer* 1986, **27**, 709
10 Gómez-Ribelles, J. L., Díaz-Calleja, R., Ferguson, R. and Cowie, J. M. G. *Polymer* 1987, **28**, 226
11 Berens, A. R. and Hodge, I. M. *Macromolecules* 1982, **15**, 756
12 Kovacs, S. J. *et al. J. Polym. Sci., Polym. Phys. Edn.* 1979, **17**, 1097
13 Narayanaswamy, O. S. *J. Am. Ceram. Soc.* 1971, **54**, 491
14 Moynihan, C. T. *et al. Ann. NY Acad. Sci.* 1976, **276**, 17
15 Hodge, I. M. *Macromolecules* 1987, **20**, 2897
16 Tool, A. Q. *J. Am. Ceram. Soc.* 1949, **39**, 403
17 Moynihan, C. T. *J. Am. Ceram. Soc.* 1976, **59**, 12
18 Williams, G. and Watts, D. C. *Trans. Faraday. Soc.* 1970, **66**, 80
19 Nedler, J. A. and Mead, R. *Comput. J.* 1965, **7**, 308
20 Gómez-Ribelles, J. L., Engn.Sci.D. Thesis, Universidad Politecnica de Valencia, 1983
21 Prest, W. M. Roberts, F. J. and Hodge, I. Proc. 12th NATAS Conf., Sept. 1980, Williamsburg, VA, pp. 119–23
22 Tribone, J. J., O'Reilly, J. M. and Greener, J. *Macromolecules* 1979, **19**, 1732
23 Cowie, J. M. G. and Ferguson, R. *Polym. Commun.* 1986, **27**, 258